Dynamic critical phenomena of mercury

2002 J. Phys.: Condens. Matter 14 L171

(http://iopscience.iop.org/0953-8984/14/6/106)

INSTITUTE OF PHYSICS PUBLISHING JOURNAL OF PHYSICS: CONDENSED MATTER

J. Phys.: Condens. Matter **14** (2002) L171–L176 PII: S0953-8984(02)31658-8

LETTER TO THE EDITOR

Dynamic critical phenomena of mercury

H Kohno and M Yao[1]

Department of Physics, Graduate School of Science Kyoto University, Sakyo-ku 606-8502, Kyoto, Japan

E-mail: yao@scphys.kyoto-u.ac.jp

Received 6 December 2001
Published 1 February 2002
Online at stacks.iop.org/JPhysCM/14/L171

Abstract

The sound attenuation in fluid mercury near the liquid–gas critical point ($T_c = 1478\,^{\circ}$C, $P_c = 167$ MPa) has been measured by means of the ultrasonic pulse–echo method at 20 and 32 MHz. We derive the entropy decay rate from the observed attenuation on the critical isochore and estimate that the dynamic critical exponent of mercury is about 3. This suggests that the dynamic critical phenomena for acoustic properties of mercury are similar to those for the insulating fluids. Using the Einstein–Kawasaki formula, we estimate also the correlation length $\xi = \xi_0(T/T_c - 1)^{-\nu}$ on the critical isochore with $\xi_0 \cong 4.1 \pm 1.0$ Å.

It is established that insulating monatomic fluids near the liquid–gas critical point belong to the universality class of the three-dimensional (3D) Ising model [1]. For expanded liquid metals, on the other hand, the metal–nonmetal (MNM) transition occurs near the critical density ρ_c and it has been speculated [2] that the intermolecular forces mediated by electrons should give rise to unique critical phenomena. The MNM transition in mercury occurs at 8–9 g cm^{-3}, which is large relative to $\rho_c = 5.8$ g cm^{-3} [3], while those in alkali metals occur at densities very close to ρ_c. In caesium, rubidium and mercury, a large deviation from the 'law of rectilinear diameters' has been observed [2], which may reflect the difference in electronic properties between the liquid and gas phases. In spite of the large diameter anomaly, the critical exponents α and β, which are deduced from the shape of the coexistence curve, have been found to be close to the 3D Ising values ($\alpha = 0.110$, $\beta = 0.325$ [4]) [2]. These findings suggest that the static critical phenomena of liquid metals belong to the same universality class as those of the simple insulating fluids. However, this does not necessarily mean that the dynamic critical phenomena of metallic fluids are the same as those of the insulating fluids. This is because one might naively question which of the so-called cluster convection [5] and the electron transport plays the more important role in the thermal conduction of the liquid metals near the critical point.

[1] Author to whom any correspondence should be addressed.

In this letter, we examine the sound attenuation in Hg near the critical point ($T_c = 1478\,^{\circ}$C, $P_c = 167$ MPa [3]) as a first systematic study of the dynamic critical phenomena in Hg; evidence for the enhanced critical sound attenuation in Hg has already been reported [6, 7]. As for the static critical phenomena, Dladla *et al* [8] have reported that the sound velocity at 4 MHz shows a minimum near the critical point. In addition to the critical attenuation, anomalous increase of the sound attenuation has been observed in the MNM transition range of Hg [9]. Thus the first purpose of this letter is to separate the critical attenuation α^{CP} from the observed sound attenuation α^{OBS} by removing the anomalous attenuation due to the MNM transition. The second purpose is to discuss the dynamic critical phenomena of Hg. Already, a considerable number of theoretical studies have been made on the sound attenuation near the liquid–gas critical point [10, 11]. Recently a new scaling function for the frequency-dependent sound attenuation has been presented [12]. Since the new scaling function is expressed as a general form with the static critical exponents α, ν and the dynamic critical exponent z, we can use it to derive the entropy decay rate of Hg on the critical isochore. We discuss whether the dynamic critical phenomena of Hg can be described with $z \approx 3$ similarly to the insulating fluids.

The sound velocity v and the sound attenuation α^{OBS} of Hg have been measured at 20 and 32 MHz in the temperature and pressure ranges up to 1600 °C and 210 MPa. We used a sample cell similar to that described in our previous paper [9, 13]: two single-crystalline sapphire rods 8 mm in diameter and 89 mm in axial length were inserted into a single-crystalline sapphire tube and used as buffer rods for transmitting the ultrasonic waves. The gap between the rods was the sample part. The cell assembly and two heaters were set in an internally heated steel high-pressure vessel which was pressurized with argon gas. The temperature of the sample part was monitored by two W–5%Re:W–26%Re thermocouples.

The sound velocity v was measured by an ultrasonic pulse transmission/echo method [14]. Two Z-cut $Pb(ZrTi)O_3$ transducers were bonded to the cold ends of the buffer rods (transducers A and B). The sound attenuation α^{OBS} can be deduced from the transmission rate T_s through the sample. In contrast to the case for ambient conditions, where T_s can be measured with varying the sample thickness l_s, it is difficult to change l_s *in situ* under high temperature and pressure. Hence, we estimate T_s as follows. We measure the voltages of the transmitted signals V_{AB} and V_{BA} in both directions. Since fairly long buffer rods are necessary for the measurements at high temperatures, the sound attenuation due to the sapphire rods is no longer negligible. Therefore, we measure also V_{AA} and V_{BB}, which are the voltages of the signals reflected from the interface between the sample and the buffer rods. We derive T_s from the ratio of the intensity of the transmitted pulse to that of the reflected pulse. In the derivation, we take into account the correction for the acoustic impedance mismatches between the buffer rods and the sample Hg. The details of the present method have been described elsewhere [9, 13].

In figure 1(a), the total sound attenuation α^{OBS} at 20 MHz, along two nearly isobaric paths, is plotted against the density. The pressure values in the figure are those at which the paths cross the critical isochore. When the density decreases, α^{OBS} increases and reaches a maximum near $\rho_c = 5.8$ g cm^{-3}. In addition to the critical attenuation, a secondary maximum is observed at 8–9 g cm^{-3}, where the MNM transition occurs (see the arrows in figure 1(a)). More detailed measurements indicate that α^{OBS} at densities larger than 8.0 g cm^{-3} is almost independent of pressure [13], which means that the temperature dependence of α^{OBS} at constant density is small. This suggests that the critical attenuation α^{CP} is negligibly small at densities larger than 8.0 g cm^{-3}. Moreover, at densities between 8.0 and 9.6 g cm^{-3}, it has been revealed that the frequency dependence of the secondary maximum is described by a Debye-type relaxation with the relaxation time $\tau = 2.2$ ns [13], which is experimental evidence for a slow-relaxation process due to the MNM transition.

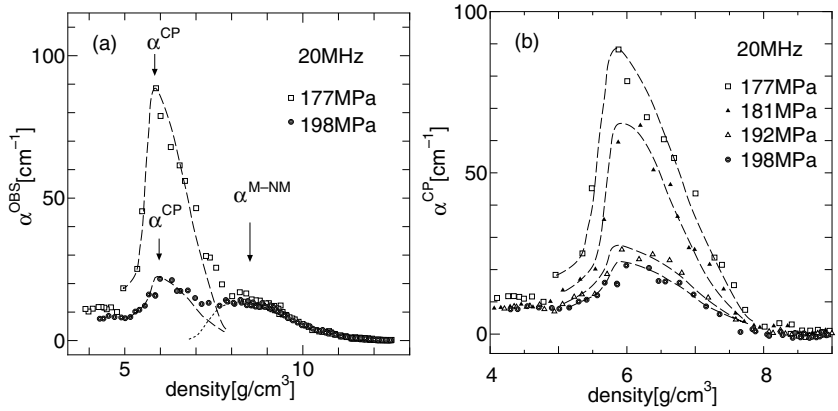

Figure 1. (*a*) The total sound attenuation α^{OBS} versus density at 20 MHz along two nearly isobaric paths. The dashed and dotted curves denote the critical attenuation α^{CP} and the anomalous attenuation in the MNM transition region α^{MNM}, respectively. (*b*) The critical attenuation α^{CP} versus density at 20 MHz along four nearly isobaric paths. The pressure values in the figure are those at which the paths cross the critical isochore. The dashed curves in the figure are guides for the eyes.

At densities smaller than 8.0 g cm^{-3}, on the other hand, α^{CP} is no longer negligible. In the density region between 7.0 and 8.0 g cm^{-3}, which is relatively far from ρ_c, the critical attenuation per wavelength α_λ^{CP} is small and should be proportional to the angular frequency ω (i.e. the hydrodynamic regime) [15]. We have separated α^{OBS} into the critical attenuation α^{CP} and the secondary maximum α^{MNM} due to the MNM transition, utilizing the difference in frequency dependence between the two components [13]. The resultant α^{MNM} becomes very small around 7.0 g cm^{-3} [13], which means that $\alpha^{OBS} \cong \alpha^{CP}$ at densities smaller than 7.0 g cm^{-3}.

The critical attenuation α^{CP} ($=\alpha^{OBS}-\alpha^{MNM}$) at 20 MHz, along four nearly isobaric paths, is plotted as a function of density in figure 1(*b*). When the density decreases, α^{CP} begins to increase around 8 g cm^{-3}, and reaches a maximum near ρ_c. The peak becomes larger as the pressure approaches P_c. To show the asymptotic behaviour of α^{CP} on approaching the critical point, the logarithm of the critical attenuation per wavelength, α_λ^{CP}, at 20 MHz on the critical isochore is plotted against the logarithm of the reduced temperature $\epsilon \equiv |T - T_c|/T_c$ (as triangles) in figure 2. We plot also the data at 32 MHz (as open circles). At temperatures close to T_c ($\epsilon < 0.03$), α^{CP} at 32 MHz was too large to be measured. On approaching the critical temperature, α_λ^{CP} increases monotonically.

Theoretical works on the critical phenomena have predicted that the critical attenuation per wavelength α_λ^{CP} should be expressed as a function of the dimensionless frequency $\omega^* = \omega/2\Gamma_\xi$ [15], where Γ_ξ is the decay rate of the entropy fluctuation with wavenumbers of order $1/\xi$. Here ξ is the correlation length. The decay rate Γ_ξ can be written as

$$\Gamma_\xi = D\xi^{-2}, \tag{1}$$

where D is the thermal diffusivity [16]. In the low-frequency limit $\omega \ll \Gamma_\xi$, α_λ^{CP} should be proportional to ω [10]. In the high-frequency limit $\omega \gg \Gamma_\xi$; on the other hand, ξ exceeds the thermal diffusion length and the perturbed thermal equilibrium cannot be restored within the period of the sound wave. Thus the frequency dependence of α_λ^{CP} should be suppressed compared to the linear dependence on ω. Recently, a new scaling function which connects the low- and high-frequency behaviours has been presented [12]. On the critical isochore, the scaling function is expressed as a universal function of ω^* with the static critical exponents α,

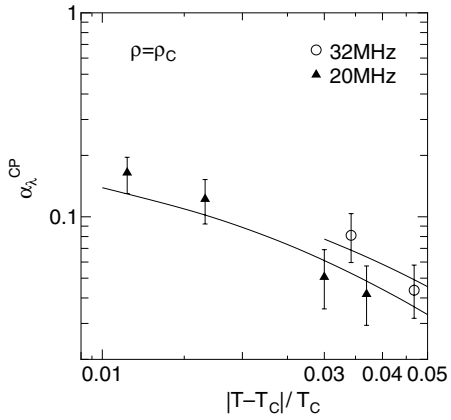

Figure 2. The critical attenuation per wavelength α_λ^{CP} versus reduced temperature $\epsilon \equiv |T - T_c|/T_c$ on the critical isochore at 20 MHz (▲) and 32 MHz (○). The solid curves represent the theoretical α_λ^{CP} [12].

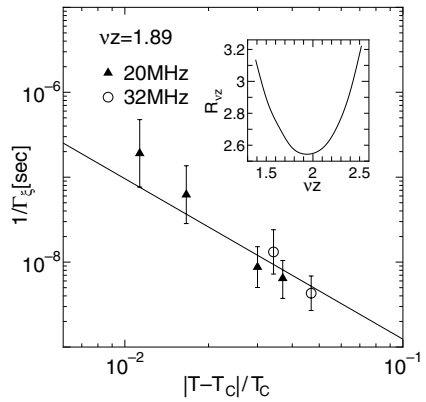

Figure 3. The inverse decay rate $1/\Gamma_\xi$ versus reduced temperature $\epsilon \equiv |T - T_c|/T_c$ on the critical isochore. The data points are obtained from the observed α_λ^{CP} shown in figure 2 with the aid of the theory [12] with $\nu z = 1.89$. The solid line represents $1/\Gamma_\xi = A\epsilon^{-\nu z}$ with $A = 1.60 \times 10^{-11}$ and $\nu z = 1.89$. Inset: the calculated residual sum $R_{\nu z}$ versus νz.

ν and the dynamic critical exponent z. Note that the relation between z and Γ_ξ is generally expressed as $\Gamma_\xi \propto \xi^{-z}$ [16].

Since reliable ξ-data have not been obtained experimentally, let us use the scaling function in discussing the dynamic critical phenomena. The exponent α of Hg has been estimated to be 0.11 [2, 17]; however, ν and z are not been known accurately. If a value of νz is given, we can derive Γ_ξ on the critical isochore from the experimental value of α_λ^{CP} by using the scaling function [12]. Since ξ is proportional to $\epsilon^{-\nu}$, the inverse of Γ_ξ is expressed as $1/\Gamma_\xi \propto \epsilon^{-\nu z}$. Thus we search for the appropriate value of νz as follows.

First we assume a value of νz and derive $1/\Gamma_\xi^{exp}$ from experimental α_λ^{CP} by using the scaling function. Next we fit the ϵ-dependence of $1/\Gamma_\xi^{exp}$ to $1/\Gamma_\xi^{cal} = A\epsilon^{-\nu z}$, where A is a fitting parameter, by least-squares fitting. We carry out the fitting with several different values of νz and calculate the residual sum $R_{\nu z}$; then we determine the most appropriate value of νz which gives the minimum $R_{\nu z}$. In figure 3, the derived $1/\Gamma_\xi^{exp}$ with $\nu z = 1.89$ is plotted

against ϵ as an example. The solid line represents the fitting result. In the fitting, we take the standard deviation represented by the error bar in the figure into account. In the inset of figure 3, the calculated $R_{\nu z}$ is plotted against νz. $R_{\nu z}$ exhibits a minimum around $\nu z = 1.93$, which corresponds to $z \approx 3$ since ν can be estimated to be 0.63 from the hyperscaling relation: $\alpha = 2 - d\nu$ [16], where d (=3) is the dimension of the system. This means that the dynamic critical phenomena for acoustic properties of Hg are similar to those for the insulating fluids. The solid curves in figure 2 represent the theoretical estimates of α^{CP} with $z = 3$ [12], which reproduce the experimental α^{CP} fairly well.

The result in this letter ($z \approx 3$) is consistent with the prediction of mode-coupling theory [15] in which the thermal diffusivity D is given by the Einstein–Kawasaki formula:

$$D = \frac{k_B T}{6\pi \eta_s \xi}, \tag{2}$$

where η_s is the shear viscosity. Combining equation (1) with (2), we estimate ξ on the critical isochore by using Γ_ξ obtained from the scaling function with $z = 3$ (see figure 3). As for η_s at the critical density, we use the extrapolated value from the experimental data [18] since the critical singularity of η_s should be very weak. The resultant ξ increases monotonically on approaching T_c and becomes about 86 Å around $\epsilon = 0.01$. We fit the ϵ-dependence of ξ by $\xi = \xi_0 \epsilon^{-0.63}$ in order to estimate the amplitude of ξ, ξ_0. The resultant ξ_0 is 4.1 ± 1.0 Å, which is larger than the typical value (~2 Å [19]) for the insulating monatomic fluids.

There may be a tendency for ξ_0 for ionic fluids to usually be larger than the values observed for non-ionic fluids [20]. Thus the present result of $\xi_0 = 4.1$ Å seems to be reasonable for Hg, which tends to be slightly ionized. The degree of ionization of Hg near ρ_c is estimated to be about 1% from the energy gap between the 6s and 6p bands [21]. It should be noted that the present result does not conflict with the Ising criticality. Indeed, weakly coulombic solutions exhibit Ising behaviour [20,22], in contrast to strongly coulombic solutions for which classical or crossover behaviour has been reported [23,24].

In summary, the sound attenuation in Hg near the liquid–gas critical point has been measured by means of the ultrasonic pulse–echo method at 20 and 32 MHz. We have observed a large increase in sound attenuation near the critical density. By use of the scaling function [12], we have derived the entropy decay rate on the critical isochore. The dynamic critical exponent has been estimated to be about 3, which is consistent with the conventional theories. This means that the dynamic critical phenomena for acoustic properties of mercury are similar to those for the insulating fluids. Using the Einstein–Kawasaki formula, we have also estimated the correlation length ξ on the critical isochore. The amplitude of ξ, ξ_0, has been estimated to be 4.1 ± 1.0 Å, which is slightly larger than that for insulating fluid.

The authors are grateful to Professor A Onuki for valuable discussions and helpful advice. We also thank Messrs Y Kajihara, Y Hiejima, N Itokawa and Miss I Hirano for collaboration in the experiments. This work was partially supported by a grant-in-aid for scientific research from the Ministry of Education, Science, Sports and Culture, Japan.

References

[1] Levelt Sengers J M H 1974 *Physica* **73** 73
[2] Hensel F and Warren W W Jr 1999 *Fluid Metals* (Princeton, NJ: Princeton University Press) ch 6
[3] Hensel F and Warren W W Jr 1999 *Fluid Metals* (Princeton, NJ: Princeton University Press) ch 1
[4] LeGuillou J C and Zinn-Justin J 1980 *Phys. Rev.* B **21** 3976
[5] Hohenberg P C and Halperin B I 1977 *Rev. Mod. Phys.* **49** 435
[6] Kozhevnikov V, Arnold D, Grodzinskii E and Naurzakov S 1996 *J. Non-Cryst. Solids* **256–60** 256

[7] Yao M, Okada K, Aoki T and Endo H 1996 *J. Non-Cryst. Solids* **256–60** 274
[8] Dladla B S, Pilgrim W C and Hensel F 1997 *Z. Phys. Chem.* **199** 295
[9] Kohno H and Yao M 1999 *J. Phys.: Condens. Matter* **11** 5399
[10] Kawasaki K 1970 *Phys. Rev.* A **1** 1750
[11] Ferrell R A and Bhattacharjee J K 1985 *Phys. Rev.* A **31** 1788
[12] Onuki A 1997 *Phys. Rev.* E **55** 403
[13] Kohno H and Yao M 2001 *J. Phys.: Condens. Matter* **13** 10 293
[14] Suzuki K, Inutake M, Fujiwaka S, Yao M and Endo H 1980 *J. Physique Coll.* **41** C8 66
[15] Kawasaki K 1976 *Phase Transitions and Critical Phenomena* vol 5a, ed C Domb and M S Green (London: Academic) ch 4
[16] Privman V, Hohenberg P C and Aharony A 1991 *Phase Transitions and Critical Phenomena* vol 14, ed C Domb and J L Lebowitz (London: Academic) ch 1
[17] Götzlaff W 1988 *PhD Thesis* University of Marburg
[18] von Tippelskirch H, Franck E U, Hensel F and Kestin J 1978 *Ber. Bunsenges. Phys. Chem.* **79** 889
[19] Sengers J V and Moldover M R 1978 *Phys. Lett.* A **66** 44
[20] Schröer W, Wiegand S, Kleemeier M and Weingärtner H 1994 *J. Phys.: Condens. Matter* **6** A157
[21] Yao M 1994 *Z. Phys. Chem.* **184** 73
[22] Naranayan T and Pitzer K S 1995 *J. Chem. Phys.* **102** 8118
[23] Zhang K C, Briggs M E, Gammon R W and Levelt Sengers J M H 1992 *J. Chem. Phys.* **97** 8692
[24] Chieux P, Jal J F, Hily L, Dupuy J, Leclercq F and Damay P 1991 *J. Physique Coll.* **1** C5 3